2, 48, Downloaded from https://chemistry-europe.online/birary.wiley.com/doi/10.1002/slc102203309 by Florida A&M University, Wiley Online Library on [04/01/2023]. See the Terms and Conditions (https://onlinelibrary.wiley.com/terms-and-conditions) on Wiley Online Library for rules of use; OA articles are governed by the applicable Creative Commons

www.chemistryselect.org

# Fabrication of Thermally Stable Sulfonated Poly(arylene ether sulfone) Containing Sulfonic Acid Based Additives for Proton Exchange Membrane Fuel Cells

D'Andra Moxey,<sup>[a]</sup> Sanjay Kumar Devendhar Singh,\*<sup>[a, b]</sup> Emily Plunkett,<sup>[c]</sup> Robert B. Moore,<sup>[c]</sup> and Natalie Y. Arnett\*<sup>[a, b]</sup>

A systematic investigations on the effect of sulfonic acid additives for the fabrication of thermally stable sulfonated poly(arylene ether sulfone) (PAES) composites for proton exchange membranes fuel cell applications were carried out. A uniform microstructure containing different concentration (1, 5 and 10 vol.%) of aromatic sulfonic acid additives (aniline-2-sulfonic acid (ASA), 3-aminobenzenesulfonic acid (ABSA) and 3-amino-4-hydroxy-benzenesulfonic acid (AHBSA)) and biphenol-based disulfonated poly(arylene ether sulfone) copolymer (PAES) as the matrix were successfully prepared. Phase segregation of the additives with sizes ranging from 1 to 2  $\mu m$  was confirmed using scanning electron microscopy (SEM). Both thermogravimetric analysis (TGA) and differential scanning

calorimetry (DSC) confirmed that additive derived PAES were thermally stable up to 400 °C. Proton conductivity of ASA-PAES membranes was found to increase gradually with ASA concentration. Among all membranes PAES-10%ASA exhibited the highest conductivity of  $0.123\pm0.01~\rm S\cdot cm^{-1}$  at 100% relative humidity. However, PAES-1%ASA and PAES-10%ABSA membranes demonstrated the lowest leaching. Water uptake, ion exchange capacity and leaching parameters were correlated to additive concentration. This study will serve as a guide for the fabrication of PAES membranes with high concentration of sulfonated group in the polymer chain with enhanced thermal stability and proton conductivity.

#### Introduction

Proton exchange membrane (PEM) fuel cells is one of the most promising energy conversion devices which has received enormous attention in recent years due to its high efficiencies, fast start-up and environmentally friendly. Proton exchange membrane fuel cells (PEMFC) operate by oxidizing various fuels such as hydrogen, methanol, or ethanol in the presence of a platinum catalyst. A typical PEMFC comprises a stack of fuel cells and auxiliary devices wherein the fuel cell stack is composed of membrane electrode assembly (MEA) and bipolar plates. The bipolar plates are electrically connected in series, and it serves as both current collector and to supply the required chemicals to the MEA assembly. On the other hand, the auxiliary devices composed of air pumps, humidifiers, manifolds and thermal controls. The most important

component of the PEM fuel cells is the electrolyte which separates the electrodes and helps to facilitate the electrochemical reactions at the electrodes during the fuel cell operation. [1a,2] In other words, PEMs simultaneously helps in the transportation of protons to the cathode, acts as a separator between oxygen and fuels, as an insulator between the electrodes and binder for the catalysts. [1a] Therefore, the efficiency of the PEMFC mainly depends on the properties of PEM. The PEMs used in the fuel cells should possess properties including low electronic conductivity, low permeability to fuel and oxidant, high proton conductivity, stable at operating temperature, resilient to chemical and electrochemical attacks, excellent water transportation, and good mechanical integrity especially during hydration states. [1b]

Commercially available membranes (Nafion®-sulfonated tetrafluoroethylene-based fluoropolymer) provide excellent fuel cell performance at room temperature in sufficient humidity condition. [3] Nafion® is considered the standard PEM as it has good chemical and physical stability, along with its high proton conductivity (0.11 S·cm<sup>-1</sup> at 25 °C).<sup>[3b,4]</sup> However, Nafion® has some limitations which includes high-cost, limited operating temperature (less than 0.1 mS·cm<sup>-1</sup> at 100 °C), environmental concerns due to the presence of fluorides in the membrane, and low glass transition temperature. [2,3b] In addition, perfluorinated membranes also suffers from high gas or methanol permeability and low durability in open circuit voltage (OCV) condition.<sup>[2,5]</sup> Hence, there is a need to develop new generations of PEM which could address these issues. Extensive research is being devoted for the development of new generations of polymeric materials that could exhibit enhanced

[b] Dr. S. K. Devendhar Singh, Prof. N. Y. Arnett Department of Chemical & Biomedical Engineering, FAMU-FSU College of Engineering, Tallahassee-32310, Florida, USA E-mail: narnett@eng.famu.fsu.edu

E-mail: narnett@eng.ramu.rsu.edu Homepage: https://eng.famu.fsu.edu/cbe/people/arnett

[c] E. Plunkett, Prof. R. B. Moore
 Department of Chemistry and Macromolecules Innovation Institute,
 Virginia Tech, Blacksburg-24061,
 Virginia, USA

Supporting information for this article is available on the WWW under https://doi.org/10.1002/slct.202203309

<sup>[</sup>a] D'A. Moxey, Dr. S. K. Devendhar Singh, Prof. N. Y. Arnett Department of Chemistry, Florida A&M University, Tallahassee-32307, Florida, USA E-mail: sd22bd@fsu.edu

fuel cell performance without affecting its mechanical/chemical stability and with reduced swelling. [1a,b, 2]

To mitigate the above mentioned issues, a variety of high performance polymer membranes are developed which includes introduction of sulfonic acid groups to poly(arylene (PAEK),<sup>[1b,6]</sup> ketones) poly(phenylene poly(phenylene oxide)[8] and polybenimidazole.[1b] Among these, poly (arylene ether)s (PAEs) has attracted much attention due to its inherent high mechanical strength, thermally stable and low cost. PAEs are well known engineering thermoplastics.  $^{[3b,9]}$  These amorphous or semi-crystalline high performance engineering thermoplastics exhibit a variety of properties like high thermal, good mechanical strength, and high glass transition temperatures. [3b,9] It was shown that the proton conductivity of poly(arylene ether ketones) could be improved (comparable to that of Nafion®) by introducing high concentration of sulfonic acid (-SO<sub>3</sub>H) groups into its microstructure by post-sulfonation or direct copolymerization techniques .[1b,9]

Direct copolymerization of sulfonated poly (arylene ether)s generally avoids the harsh post-sulfonating reactions and allows changes to the sulfonic acid concentrations to occur by simple nucleophilic aromatic substitution reaction with sulfonated monomers easily and reproducibly into the poly (arylene ether)s backbone.  $^{[10]}$  Typically, the sulfonic acid salt (-SO  $_{\!3}M$ where M = metal from base used) exhibit minimum membrane swelling but very low water performance and proton conductivity.[10a,11] To increase the performance of these membranes, different acidification methods are utilized to convert the -SO<sub>3</sub>M to -SO<sub>3</sub>H allowing for proton conduction to occur.[12] Hence, most studies on sulfonated poly (arylene ether)s PEM film have focused primarily on the acidified membranes.[12-13] In addition, high sulfonation levels, called percolation limit results in a decrease in PEM performance due to a loss in mechanical strength and extreme swelling at 50% sulfonation which affects the permeability in acidified poly (arylene ether)s membranes.<sup>[12–13]</sup> Therefore, novel synthetic methods and modifications to membrane fabrication procedures are being developed to minimize the percolation limitations while maintaining its fuel cell performance to that of Nafion<sup>®</sup>.<sup>[10a,13]</sup>

Physically blended sulfonated additives (sulfonated poly(arylene ether sulfone) (PAES)) into polymers offer an attractive alternate route to prepare PEM membranes while minimizing the negative effects related to high sulfonation levels in polymer synthesis.[10a] Blending bisphenol S polymers with sulfonated additives allows for high sulfonation levels within PAES structures without sacrificing the mechanical stability and proton conductivity of the membranes.[10a,14] Improvements to copolymer-copolymer miscibility can be achieved by promoting intermolecular interactions such as hydrogen bonding, dipole-dipole interaction, acid-base interactions, and covalent crosslinking.[14-15] As the bond strength of each interaction becomes stronger the polymer miscibility may be increased. Self-crosslinking was observed in sulfonated PEEK films dissolved in DMSO.[16] Additional crosslinking abilities were also exhibited when the sulfonated PEEK was blended with PAES.[10a,14] It was found that the power density of these membranes was higher compared to that of Nafion® 212 at 80 °C under 100% relative humidity. [10a,14] Furthermore, the use of DMSO to prepare sulfonated PAEK films also demonstrated high proton conductivity of 0.15 S·cm<sup>-1</sup> at 65 °C. [6] Similarly, sulfonated poly(arylene ether ketones) polymers bearing -COOH groups for direct methanol fuel cell applications crosslinked in DMSO were found to exhibit the proton conductivity of 0.197 S·cm-1 (higher than that of Nafion®: 0.146 S·cm-1).[17] Therefore, it is evident that the utilization of PAES-additive composite membranes prepared in DMSO could assist in crosslinking.[10a,14] In this study, PAES composite membranes were fabricated in DMSO using three sulfonated additives: 3-aminobenzenesulfonic acid (ABSA), 3-amino-4-hydroxy-benzenesulfonic acid (AHBSA) and aniline-2-sulfonic acid (ASA) (Figure 1).

$$H = \left\{ \begin{array}{c} & & & & \\ & & & \\ & & & \\ & & & \\ \end{array} \right\} = \left\{ \begin{array}{c} & & & \\ & & & \\ \end{array} \right\} = \left\{ \begin{array}{c} & & & \\ & & & \\ \end{array} \right\} = \left\{ \begin{array}{c} & & & \\ & & & \\ \end{array} \right\} = \left\{ \begin{array}{c} & & & \\ & & & \\ \end{array} \right\} = \left\{ \begin{array}{c} & & & \\ & & & \\ \end{array} \right\} = \left\{ \begin{array}{c} & & & \\ & & & \\ \end{array} \right\} = \left\{ \begin{array}{c} & & & \\ & & & \\ \end{array} \right\} = \left\{ \begin{array}{c} & & & \\ & & & \\ \end{array} \right\} = \left\{ \begin{array}{c} & & & \\ & & & \\ \end{array} \right\} = \left\{ \begin{array}{c} & & & \\ & & & \\ \end{array} \right\} = \left\{ \begin{array}{c} & & & \\ & & & \\ \end{array} \right\} = \left\{ \begin{array}{c} & & & \\ & & & \\ \end{array} \right\} = \left\{ \begin{array}{c} & & & \\ & & & \\ \end{array} \right\} = \left\{ \begin{array}{c} & & & \\ & & & \\ \end{array} \right\} = \left\{ \begin{array}{c} & & & \\ & & & \\ \end{array} \right\} = \left\{ \begin{array}{c} & & & \\ & & & \\ \end{array} \right\} = \left\{ \begin{array}{c} & & & \\ & & & \\ \end{array} \right\} = \left\{ \begin{array}{c} & & & \\ & & & \\ \end{array} \right\} = \left\{ \begin{array}{c} & & & \\ & & & \\ \end{array} \right\} = \left\{ \begin{array}{c} & & & \\ & & & \\ \end{array} \right\} = \left\{ \begin{array}{c} & & & \\ & & & \\ \end{array} \right\} = \left\{ \begin{array}{c} & & & \\ & & & \\ \end{array} \right\} = \left\{ \begin{array}{c} & & & \\ & & & \\ \end{array} \right\} = \left\{ \begin{array}{c} & & & \\ & & & \\ \end{array} \right\} = \left\{ \begin{array}{c} & & & \\ & & & \\ \end{array} \right\} = \left\{ \begin{array}{c} & & & \\ & & & \\ \end{array} \right\} = \left\{ \begin{array}{c} & & & \\ & & & \\ \end{array} \right\} = \left\{ \begin{array}{c} & & & \\ & & & \\ \end{array} \right\} = \left\{ \begin{array}{c} & & & \\ & & & \\ \end{array} \right\} = \left\{ \begin{array}{c} & & & \\ & & & \\ \end{array} \right\} = \left\{ \begin{array}{c} & & & \\ & & & \\ \end{array} \right\} = \left\{ \begin{array}{c} & & & \\ & & & \\ \end{array} \right\} = \left\{ \begin{array}{c} & & & \\ & & & \\ \end{array} \right\} = \left\{ \begin{array}{c} & & & \\ & & & \\ \end{array} \right\} = \left\{ \begin{array}{c} & & & \\ & & & \\ \end{array} \right\} = \left\{ \begin{array}{c} & & & \\ & & & \\ \end{array} \right\} = \left\{ \begin{array}{c} & & & \\ & & \\ \end{array} \right\} = \left\{ \begin{array}{c} & & & \\ & & \\ \end{array} \right\} = \left\{ \begin{array}{c} & & & \\ & & \\ \end{array} \right\} = \left\{ \begin{array}{c} & & & \\ & & \\ \end{array} \right\} = \left\{ \begin{array}{c} & & & \\ & & \\ \end{array} \right\} = \left\{ \begin{array}{c} & & & \\ & & \\ \end{array} \right\} = \left\{ \begin{array}{c} & & & \\ & & \\ \end{array} \right\} = \left\{ \begin{array}{c} & & & \\ & & \\ \end{array} \right\} = \left\{ \begin{array}{c} & & & \\ & & \\ \end{array} \right\} = \left\{ \begin{array}{c} & & & \\ & & \\ \end{array} \right\} = \left\{ \begin{array}{c} & & & \\ & & \\ \end{array} \right\} = \left\{ \begin{array}{c} & & & \\ & & \\ \end{array} \right\} = \left\{ \begin{array}{c} & & & \\ & & \\ \end{array} \right\} = \left\{ \begin{array}{c} & & & \\ & & \\ \end{array} \right\} = \left\{ \begin{array}{c} & & & \\ & & \\ \end{array} \right\} = \left\{ \begin{array}{c} & & & \\ \end{array} \right\} = \left\{ \begin{array}{c} & & \\ & & \\ \end{array} \right\} = \left\{ \begin{array}{c} & & \\ \end{array} \right\} = \left\{ \begin{array}{c} & & \\ & & \\ \end{array} \right\} = \left\{ \begin{array}{c} & & \\ & & \\ \end{array} \right\} = \left\{ \begin{array}{c} & & \\ & & \\ \end{array} \right\} = \left\{ \begin{array}{c} & & \\ & & \\ \end{array} \right\} = \left\{ \begin{array}{c} & & \\ & & \\ \end{array} \right\} = \left\{ \begin{array}{c} & & \\ & & \\ \end{array} \right\} = \left\{ \begin{array}{c} & & \\ & & \\ \end{array} \right\} = \left\{ \begin{array}{c} & & \\ & & \\ \end{array} \right\} = \left\{ \begin{array}{c} & & \\ & & \\ \end{array} \right\} = \left\{ \begin{array}{c} & & \\ & & \\ \end{array} \right\} = \left\{ \begin{array}{c} & & \\ & & \\ \end{array} \right\} = \left\{ \begin{array}{c} & & \\ \end{array} \right\} = \left\{ \begin{array}{c} & & \\ & \\ \end{array} \right\} = \left\{ \begin{array}{c} & & \\ \end{array} \right\} = \left\{ \begin{array}{$$

Biphenol Based Poly(arylene ether sulfone) Copolymers

Aniline-2-sulfonic acid (ASA)

3-aminobenzenesulfonic acid (ABSA)

3-amino-4-hydroxybenzene sulfonic acid (AHBSA)

Figure 1. Chemical Structures of Biphenol Based Poly(arylene ether sulfone) Copolymers and additives utilized in the preparation of polymer electrolyte membranes



To understand the contribution of sulfonated additives to the PEM performance of unacidified PAES polymers were used. PAES is expected to provide excellent thermal stability and good mechanical properties<sup>[18]</sup> while varying the ratio of each sulfonated additive in the film will allow modifiable water and fuel cell performance properties to be achieved. Additionally, the effect of high sulfonation and its effects on the percolation threshold limits in PAES membranes have also been carried out. Customization of PEM with suitable physical and mechanical properties and improved proton conductivity performances are possible from the preparation of these composite.

#### **Experimental Section**

#### Materials

4,4'-Disulfonated biphenol- based poly (arylene ether sulfone) random copolymer (PAES) was purchased commercially from Akron Polymer Systems, Akron, OH, USA. Dimethyl sulfoxide (DMSO,  $\geq$  99.9%), 3-aminobenzene sulfonic Acid (ABSA) ( $\geq$  97%), 3-amino-4-hydroxybenzene sulfonic Acid (AHBSA) ( $\geq$  95%) and aniline-2-sulfonic acid (ASA) ( $\geq$  95%), were all purchased from Sigma-Aldrich, St. Louis, MO, USA and was used as such without further purification. Sodium hydroxide was supplied by Oakwood Chemical, N. Estil, SC, USA.

### Preparation of PAES and PAES-additive composite membranes

PAES standard membranes were prepared by dissolving PAES (salt form) in DMSO (5% w/v solution). The solutions were filtered and then casted onto glass plates and dried under a heating lamp at 60°C for 24 h. To prepare PAES-XX (XX denotes additives like ASA, ABSA or AHBSA) composite membranes, separate 5% w/v solutions of PAES and each additive were prepared in DMSO. These solutions were filtered and allowed to stir at 50°C for 30 minutes prior to membrane fabrication. The additive solutions of 1, 5, and 10 vol.% were introduced into PAES solutions and the mixtures were stirred for 2 h. Casting the composite membranes were achieved using the same casting procedure as discussed previously.

#### Characterization

#### Structural Analysis using FTIR

The functional group present in blended films were determined by using attenuated total reflectance-Fourier transmission infrared (ATR-FTIR) Spectroscopy supplied by Bruker Optik Alpha FTIR Spectrometer with a platinum ATR attachment was used. The spectrum was measured for each sample from 400 to 4000 cm<sup>-1</sup> and averaged of 300 scans are presented in this study.

#### Thermal Analysis

Thermogravimetric analysis (TGA) was used to measure the change in the mass of a sample as a function of temperature at constant pressure to determine thermal stability and the dehydration processes. TGA of dried films were carried out in a TA Q50 up to 500 °C with the heating rate of 10 °C min<sup>-1</sup> in nitrogen atmosphere (flow rate: 60.0 mL min<sup>-1</sup>). Thermal transitions of the composite films were carried out using differential scanning calorimetry (DSC)

(TA Q250) in  $N_2$  flow. Approximately 7–10 mg of dried PAES-additive membranes were initially equilibrated to 100 °C in DSC in  $N_2$  flow. Subsequently, the films were cooled down to 30 °C and the second heat of the DSC run was recorded from 30 to 300 °C at a rate of 10 °C min<sup>-1</sup> under a nitrogen flow rate of 40 mL min<sup>-1</sup>. The glass transition temperature ( $T_g$ ) of the samples were calculated at the midpoint of the slope change in the DSC curve.

#### Water Tests

The water uptake of the dried PAES-additive membranes was carried out by weighing their corresponding films (dry weight). The dried PAES-additive membranes were placed in 50 mL of water at 25 °C for 24 h. The wet films were blotted to remove excess water and water droplets from the films. The weight changes were measured to observe the extent of water uptake. Later, these films were dried overnight at 100 °C in a vacuum oven and re-weighed to determine the amount of sulfonated additive leached from the membrane. The leached amount of additive was also determined by evaporating the remaining water and re-weighing the container with any residue left behind. The following equation (Eq.1) was used to calculate the water uptake/leaching percentage of each film:

$$Water \ uptake \ (\%) = \frac{Wt_{wet} - \ Wt_{dry}}{Wt_{dry}} \ \times \ 100 \eqno(1)$$

Where  $Wt_{\text{wet}}$  and  $Wt_{\text{dry}}$  are the weights of wet and dry films, respectively.

#### Ion Exchange Capacity (IEC)

Titration method was used to determine the weight-based IEC of the films. The films were soaked in 3 M NaCl solution for 24 h to allow the  $\rm H^+$  ions in the films to be replaced by Na $^+$  ions. The liberated  $\rm H^+$  ions are titrated with 0.1 M NaOH solution using phenolphthalein as an indicator. Eq. 2 was used to compute the weight-based IEC of each film:

$$IEC = \frac{Volume \ of \ NaOH \ consumed \ \times \ molarity \ of \ NaOH}{mass \ of \ dry \ film}$$
 (2) 
$$(meq.g^{-1})$$

#### **Proton Conductivity**

The proton conductivity of the films was carried out using a SolarTron SI 1287 potentiostat. Before conducting the measurement, all the films were separately equilibrated in the deionized water for 24 h. Followed by the equilibrated films were rinsed with water and placed in a 4-point clamp. The clamped films were submerged in water and ran for three sequential cyclic voltammetry experiments. The sweep was run in open circuit potential with the scan rate of 10 mV s<sup>-1</sup> in cycles between the range -0.25 to 0.25. Resistance (R) of the films were elucidated from the CV, which in turn was used to determine the conductivity (σ). The following equation was used to determine the conductivity (Eq. 3):

$$\sigma = \frac{L}{t \times w \times R} \tag{3}$$



Where L is distance between the electrodes (0.425 cm), t and w are the thickness and width of the films, respectively.

#### Microstructural analysis

Microstructural and morphological analysis of the films was carried out using Phenom XL G2 scanning electron microscopy (SEM) supplied by DOW\*. The films were carefully cut into defined size and were coated with Au to a thickness of 7 nm using Cressington Sputter Coater 108 to minimize the surface charging effect.

#### **Results and Discussion**

PAES composite membranes were prepared by dissolving 4,4'-disulfonated biphenol- based poly (arylene ether sulfone) random copolymer in DMSO. No pre- or post-acidification were carried out on the films to convert the salt form to an acid form which is required for enhanced proton conductivity to occur. Instead, PAES remained in the salt form during the fabrication and analysis of the films to demonstrate the effect of different concentrations of ASA, ABSA or AHBSA on the membrane performance.

#### FTIR analysis

Figure 2 shows the FTIR spectrum of additives used ASA, ABSA, AHBSA and their corresponding membranes prepared by using 1, 5 and 10 vol.% of additives. Figure 2 also shows the FTIR spectrum of PAES (with no additives). FTIR spectrum of ASA, ABSA and AHBSA shows the N—H stretching vibration approx-

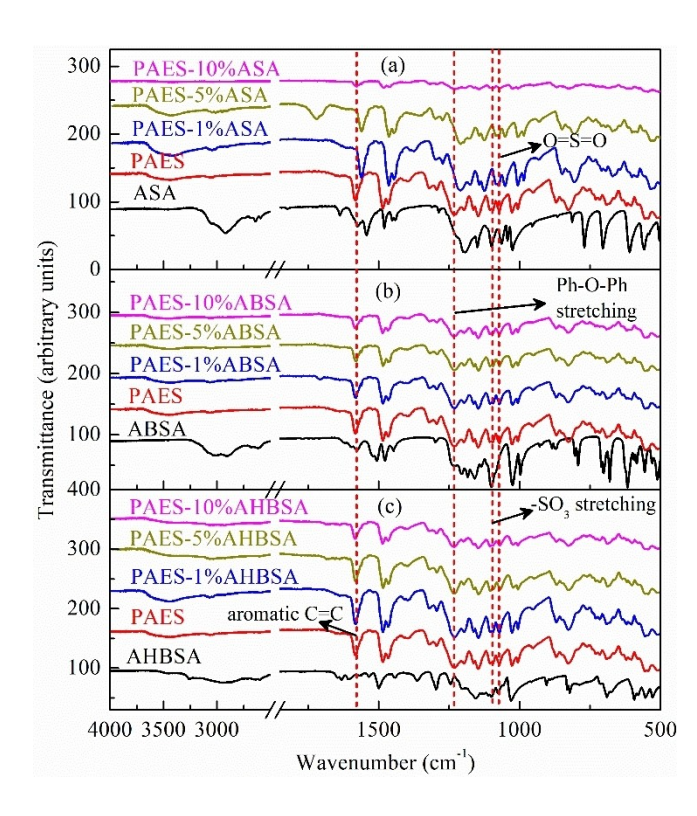


Figure 2. FTIR spectrum of additives and PAES-additive membranes

imately at 3080 cm<sup>-1[19]</sup> while the aromatic C=C and C-H bonds were found to appear at 1638 cm<sup>-1</sup> and 1480 cm<sup>-1</sup> respectively. The C-N mode appears approximately at 1434 cm<sup>-1</sup>.<sup>[20]</sup> The sulfonate group is confirmed by the presence of S=O stretching peak at 1096 cm<sup>-1</sup>.[20-21] The stretching vibrational peaks observed at 767 cm<sup>-1</sup> and 615 cm<sup>-1</sup> are attributed to the presence of S-O and C-S respectively.[21] These bands confirm the presence of  $SO_3^-$  attached to the benzene ring of ASA, ABSA and AHBSA additives. A broad peak around 3500 cm<sup>-1</sup> was observed in AHBSA which confirms the presence of hydroxyl group. FTIR spectrum of PAES reveals the presence of minor but broad peak around 3500 cm<sup>-1</sup> which could be attributed due to O-H stretching vibration. The characteristic peaks appearing at 1031 and 1097 cm<sup>-1</sup> confirms the presence of symmetric and asymmetric stretching of  $SO_3^{-,[22]}$  A strong peak appearing at 1231 cm<sup>-1</sup> is due to the presence of aromatic ether linkage (Ph-O-Ph stretching).[23] Similarly, FTIR spectrum of PAES blended with 10 vol.% additivities are shown in Figure 2. The absence of any peak at  $1700\ cm^{-1}$  confirms the absence of benzenoid and quinoid moieties in the membranes.[22-23] The presence of a strong peak around 1230 cm<sup>-1</sup> in PAES, PAES-XX additives confirms the presence of aromatic ether linkage. [23] The S=O stretching peak appearing approximately at 1096 cm<sup>-1</sup> confirms the presence of sulphonate group<sup>[20-21]</sup> in the membranes while the S-O and C-S stretching vibrational peaks are observed  $\approx$  767 and 615 cm<sup>-1</sup>, respectively. [21] Apart from these peaks, characteristic peaks corresponding to aromatic C-H could also be observed at 1480-1486 cm<sup>-1</sup>. FTIR spectrum of membranes could not detect substantial signal corresponding to N-H stretching vibration which could be due to its low concentration, however, minor but broad O-H stretching vibration peaks could be observed around 3500 cm<sup>-1</sup> which corresponds to presence of residual moisture in the membranes. Therefore, from the above discussion, it could be concluded that the sulfonic acid and ether linkage groups are intact in the membranes. The former plays a vital role during proton exchange process while the latter helps the membranes to be intact.

#### SEM analysis and transparency

Scanning electron microscopy (SEM) examination of PAES-additive membranes was carried out to investigate the effect of different sulfonated additivities and its varying degree of concentration on its microstructure (Figure 3 and Figure S2). SEM analysis revealed that PAES membranes were smooth, crack-free and devoid of pores (Figure 3 and Figure S2). Microstructural investigation of PAES-ASA membranes confirmed that the sulfonated additivities (ASA) were miscible up to 10 vol.% in PAES polymer and no phase separation was observed. On the other hand, PAES-ABSA and PAES-AHBSA membranes exhibited phase separation from 5 vol.% additive addition. Backscattered SEM images shows signs of immiscibility with the appearance of either needle-like structures in PAES-5%ABSA and PAES-10%ABSA membranes or spiky particles in PAES-5%AHBSA and PAES-10%AHBSA. From Figure 3

Chemistry Europe

European Chemical Societies Publishing

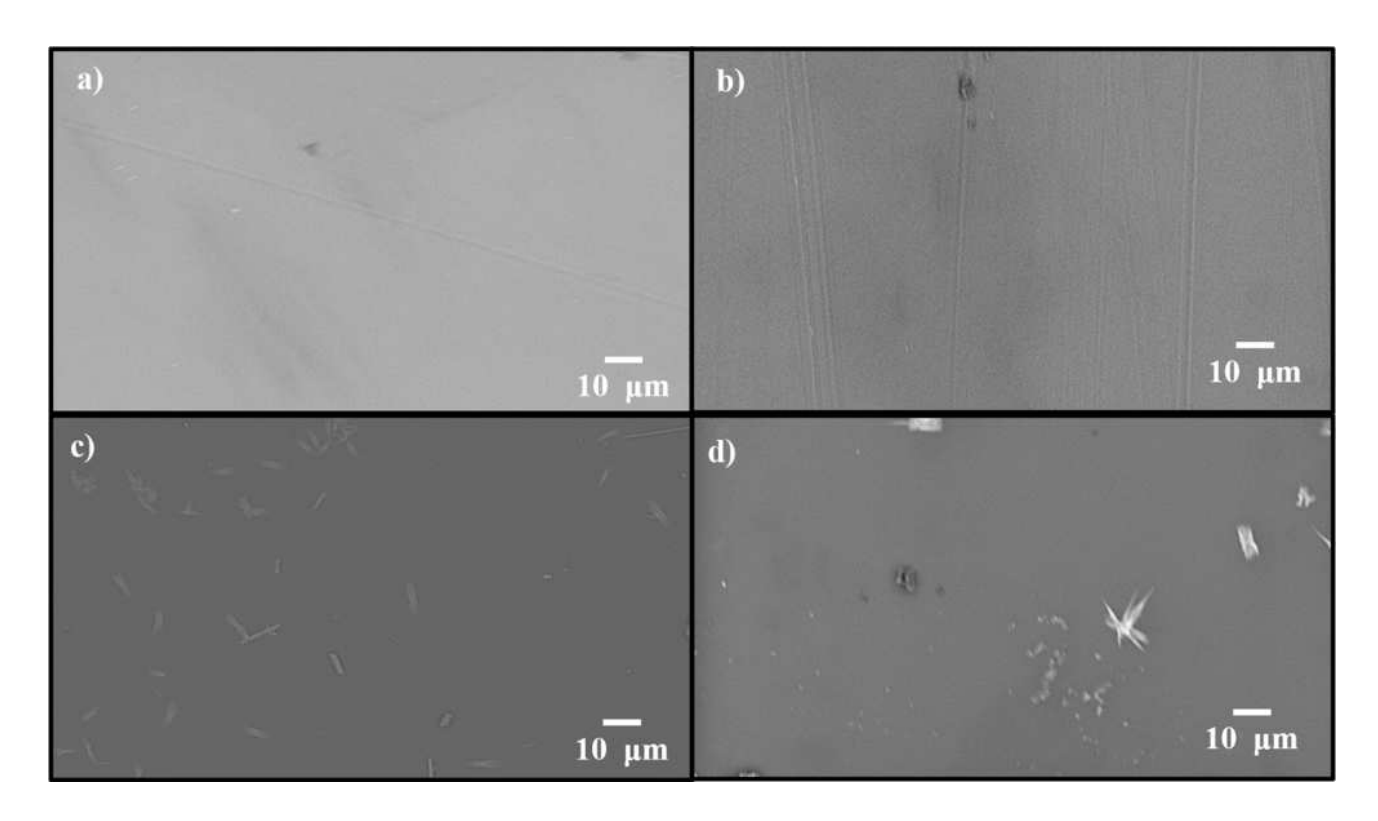


Figure 3. SEM images of membranes: (a) PAES and (b) PAES-5 %ASA, (c) PAES-5 %ABSA and (d) PAES-5 %AHBSA

and Figure S2 it is evident that the phase separated particles are randomly distributed in the PAES polymer matrix. Similarly, it was also observed that the phase separated particle sizes increase with the AHBSA additive concentration which could possibly be due to the formation of ionic aggregates, a common phenomenon observed in sulfonated PEM membranes.<sup>[21,24]</sup> From the above discussion, it is evident that the increase in AHBSA additive concentration (hydroxyl group) promotes the formation of larger hydrophilic aggregates compared to that of PAES-ASA and PAES-ABSA membranes.<sup>[24]</sup> These structures were found to impart some positive effects in proton conductivity in PAES-10%AHBSA membranes as it provides better ionic pathways for proton conduction.<sup>[24]</sup>

Table 1 shows the visual examination of pristine and PAES-additive membranes (where T-indicates visual transparency). It was found that all the membranes prepared in this study were visually transparent. However, changes in the membrane color intensity could be observed with additive type and change in their concentrations. The visual clarity is an indication of effective miscibility between sulfonated additives and PAES polymer.

Table 1. Summary of membrane tests.										
S. No.	Membrane	C (%)	T <sub>g</sub> (°C)	T <sub>m</sub> (°C)	VT	IEC (meq∙g <sup>-1</sup> )	WU (wt.%)	L (%)	Conductivity $(S \cdot cm^{-1})$	
		1	-	-	Т	0.13	4.3	11	0.103 ± 0.005	
1.	PAES-ASA	5	170	185	Т	0.54	5.0	13	$0.106 \pm 0.006$	
		10	124	162	Т	0.82	8.2	16	$0.123 \pm 0.009$	
		1	-	158	T	0.26	7.0	10	$0.071 \pm 0.003$	
2.	PAES-ABSA	5	113	198	T	0.43	5.5	13	$0.067 \pm 0.002$	
		10	116	149	T	0.48	2.0	9	$0.103 \pm 0.007$	
		1	_	-	T	0.16	9.1	9	$0.086 \pm 0.006$	
3.	PAES-AHBSA	5	-	131	T	0.37	7.2	14	$0.090 \pm 0.006$	
		10	167	178	Т	1.08	4.8	18	$0.083 \pm 0.004$	
4.	PAES	-	170	-	Т	0.35	6.6	9	$0.00274 \pm 0.00002$	

Where  $T_g$  and  $T_m$  are glass transition temperature and melting point respectively. M – membranes, C – composition, VT – Visual transparency, T – transparent, WU – water uptake, L – Leaching and IEC – Ion exchange capacity



# Thermal properties and membrane performance

#### Thermogravimetric analysis

Figure 4 shows the thermal stability comparisons of additives and PAES-additive composite membranes carried out by using TGA. It was carried out to evaluate the effect the sulfonated additive type and its concentration on the thermal stability of the membranes up to 490 °C. Figure 4 shows the TGA curves of PAES membrane without additive and PAES with 10 vol.% different additives (ASA, ABSA and AHBSA). Figure 4a reveals two thermal events with minor weight loss due to dehydration up to 200 °C. The first thermal event results in weight loss of about 15 wt.% between the temperature range 200-350 °C while the second thermal event observed above 350°C, resulted in weight loss of about 10 wt.%. In general, the initial slight mass loss of about 1-2 wt.% is attributed to dehydration (80-200 °C) while the second mass loss are due to degradation of the sulfonic group to SO<sub>3</sub>. The third mass loss takes place due to the decomposition of polymer backbone.

Figure 4a shows the thermogravimetric analysis of PAES and PAES with 10 vol.% additive membranes. PAES and PAES-10% additives films exhibited the dehydration mass loss of

about 1.0 wt.% up to 200 °C (except PAES-10 %ABSA). PAES-10%ABSA exhibited the dehydration mass loss up to 218°C which could probably be due to coupled effects viz., intermolecular hydrogen bonding and due to the presence of extra bound water molecules in the membrane.[17,25] The dehydration mass loss observed in this study are much less compared to PAES membranes reported in other studies. [26] PAES film was found to exhibit the mass loss of  $\approx$  6.6 wt.% due to the degradation of sulfonic acid group between the temperatures 200 to 305 °C. The polymer backbone was found to degrade from 438 °C (Figure 4a). On the other hand, PAES membranes with 10 vol.% additive exhibited the sulfonic acid group degradation from 190 to 412 °C (Figure 4a). The mass loss due to sulfonic acid group excluding the dehydration loss was found to 7.5, 12.7 and 13.5 wt.% for PAES-10%ABSA (219 to 412 °C), PAES-10 %AHBSA (190 to 398 °C) and PAES-10 %ASA (209 to 394°C) membranes, respectively. A closer look at second weight loss reveals that the sulfonic acid group weight loss is proportional to the additive concentration and the observation and is in-line to previous reports. [25] However, PAES-10%ABSA membrane was found to exhibit the lowest sulfonic acid weight loss between the temperatures of 190 to 412 °C. The temperature span is much higher compared to that

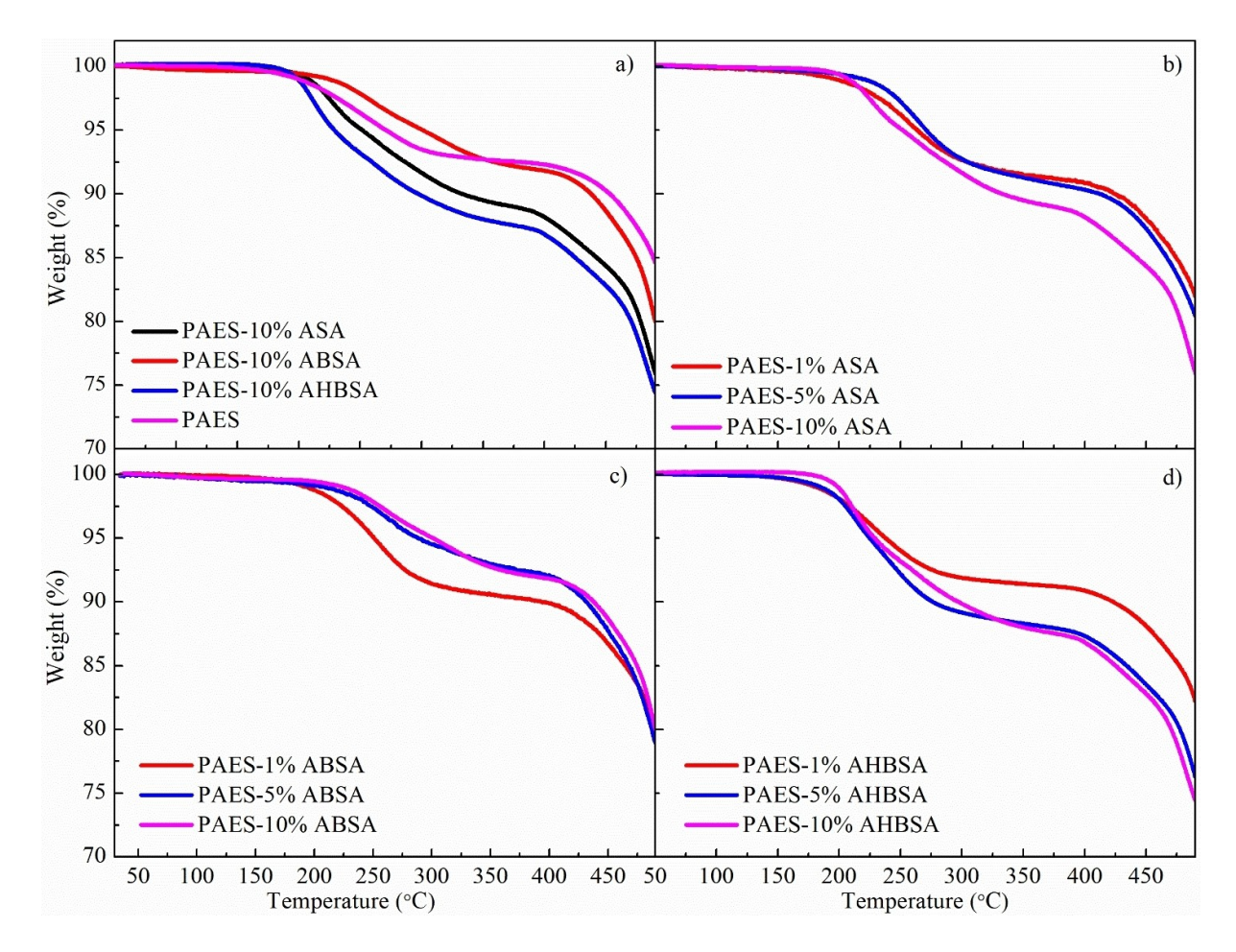


Figure 4. Thermogravimetric analysis of (a) pristine PAES and PAES-additive membranes with 10 vol.% concentration, and comparison of (b) PAES-ASA membranes, (c) PAES-ABSA membranes and (d) PAES-AHBSA membranes with different additive concentrations



of other PAES membranes with 10 vol.% additive which indicates that the sulfonic acid degradation is slow when ABSA additives are used. Above 450 °C, all PAES membranes with 10 vol.% additives displayed excess mass loss due to decomposition of the polymer backbone which is in line with literature reported values. [25-26]

Figure 4b-d and Figure S1 shows the thermogravimetric analysis of membranes with 1, 5 and 10 vol.% of additives and their corresponding pure additives. This study was carried out to understand the effect of additive concentration on the thermal stability of the PAES membranes. As expected, two thermal events were observed with initial mass loss up to 325 °C due to decomposition of sulfonic acid group, followed by mass loss due to breaking of polymer backbone. It was observed that the onset temperature for sulfonic acid loss for PAES-1%ASA, PAES-5%ASA and PAES-10%ASA were found to be 215, 234 and 217 °C respectively. These results confirm that the thermal decomposition temperature of sulfonic acid group in membranes have improved compared to that of PAES membranes, however, beyond 5 vol.% ASA additives in PAES membranes do not bring any substantial change. Figure S1 also shows the thermogram curve of pure ASA overlapped with PAES-additive membrane for comparison. Pure ASA demonstrated the initial mass loss of about 6.5 wt.% between the temperatures 283 to 338°C due to the decomposition of sulfonic acid group. Further, increase in temperature from 338°C and 373°C resulted in enormous mass loss of about 56.5 wt.% due to the decomposition of the organic moiety. From the above discussion, it could be concluded that excess concentration of ASA (above 5 vol. %) additives to PAES do not bring any substantial change in sulfonic acid group stability. However, these results confirms that the thermal stability of PAES membranes has greatly improved due to the addition ASA additives.

Similar, studies were carried out for other PAES-additive membranes (Figure 4c-d). Wherein, it was observed that the onset temperature of sulfonic acid group decomposition increases with the increase in concentration of ABSA additives compared to that of PAES membranes (Figure 4c). PAES/ABSA membranes exhibited linear increase in onset temperature with additive concentration viz., PAES-1%ABSA: 210°C, PAES-5% ABSA: 225 °C and PAES-10 % ABSA: 228 °C. The onset temperature for polymer degradation was found to be between 421-427 °C for PAES-ABSA membranes (Figure 4c). On the other hand, PAES/AHBSA membranes showed slightly lowered onset sulfonic acid degradation temperature at all additive concentrations (193°C) compared to that of plain PAES films ( pprox 200 °C) (Figure 4d). An interesting observation was that the thermal stability of PAES-AHBSA membranes followed an inversely correlation with the AHBSA concentration (PAES-1% AHBSA: 417 °C, PAES-5 %AHBSA: 397 °C and PAES-10 %AHBSA: 377 °C) which could probably be due to the side-group elimination process. In other words, the additive functional groups (-SO<sub>3</sub>H, -OH and -NH<sub>2</sub>) forming bonds with the PAES main chain reacts with each other to form volatile products at lower temperature. Hence, it results in lowering of thermal stability of PAES membrane with AHBSA concentration. Thermogravimetric analysis of PAES-XX additive membranes confirmed that the thermal stability of the polymers has greatly improved due to the presence of additives and it has also helped to delayed the onset sulfonic acid group decomposition temperature. These results ascertain that PAES-additive composite membrane polymers are better compared to that of Nafion® membranes (400°C). [9,26a] Further, the decomposition temperatures of membranes derived in this study are in-line to those reported in the literature on sulfonated poly(arylene ketone) membranes. Therefore, it could be concluded that the fabricated membranes (PAES-additive membranes) are comparable with the PAES membranes reported in the literature. [3a,25-26,27]

#### Differential scanning calorimetry (DSC) analysis

DSC could be used to study the thermal properties of PEM membrane structure to predict the degree of miscibility, degree of crystallization, glass transition temperature, and kinetics of a reaction.[28] PAES and PAES-additive membranes that are used in this study are amorphous and composed of free volumes, therefore addition of additives not only affects the membrane structure at the molecular level but also decreases their corresponding glass transition temperature. [28b] Figure 5 shows the DSC analysis of pure additives, PAES film and PAES-additive films from room temperature to 300 °C. The glass transition temperature of PAES membrane was found to be 170 °C (inset Figure 5) followed by an endothermic curve with peak temperature at 241°C which could probably be due to melting of polymer. Figure 5a shows the DSC curve of PAES and its corresponding membranes with 10 vol.% additives. In this study, it was observed that the PAES-additive membranes undergo molecular relaxation which is confirmed by appearance of endothermic peak at the end of a  $T_{\alpha}$  in DSC analysis (Figure 5). This type of molecular relaxation i.e., endothermic transition at the end of  $T_{\alpha}$  are known to occur in cross-linked polymers and are strongly dependent on the processing methods. [29] Therefore, the stresses built in PAES-additive membranes are relieved as the cross-linked polymers undergoes transition from rigid to a flexible structure as endotherm during glass transition stage.  $^{[29]}$  The  $T_q$  and melting point of PAES membranes with 10 vol.% additives were observed at 124, 116 and 167  $^{\circ}$ C and 162, 149 and 178  $^{\circ}$ C respectively. These values confirm that additives have clearly affected the thermal properties. A minor exothermic hump was observed for these membranes are around 226 to 270°C which are due to the polymer membrane degradation. These observations are in-line with thermogravimetric mass loss due to aromatic sulphonyl group degradation (Figure 4). Studies carried out on sulfonated poly(arylene ether sulfone) embedded with silicotungstic acid revealed that the mass loss observed approximately at 280 °C are due to sulfonic acid degradation.<sup>[30]</sup> The above results confirms that the membranes degradation due to aromatic sulfonic acid groups overlaps with the literature and the addition of AHBSA gives better thermal properties compared to that of other membranes with 10 vol.% additive content.

Chemistry Europe

European Chemical Societies Publishing

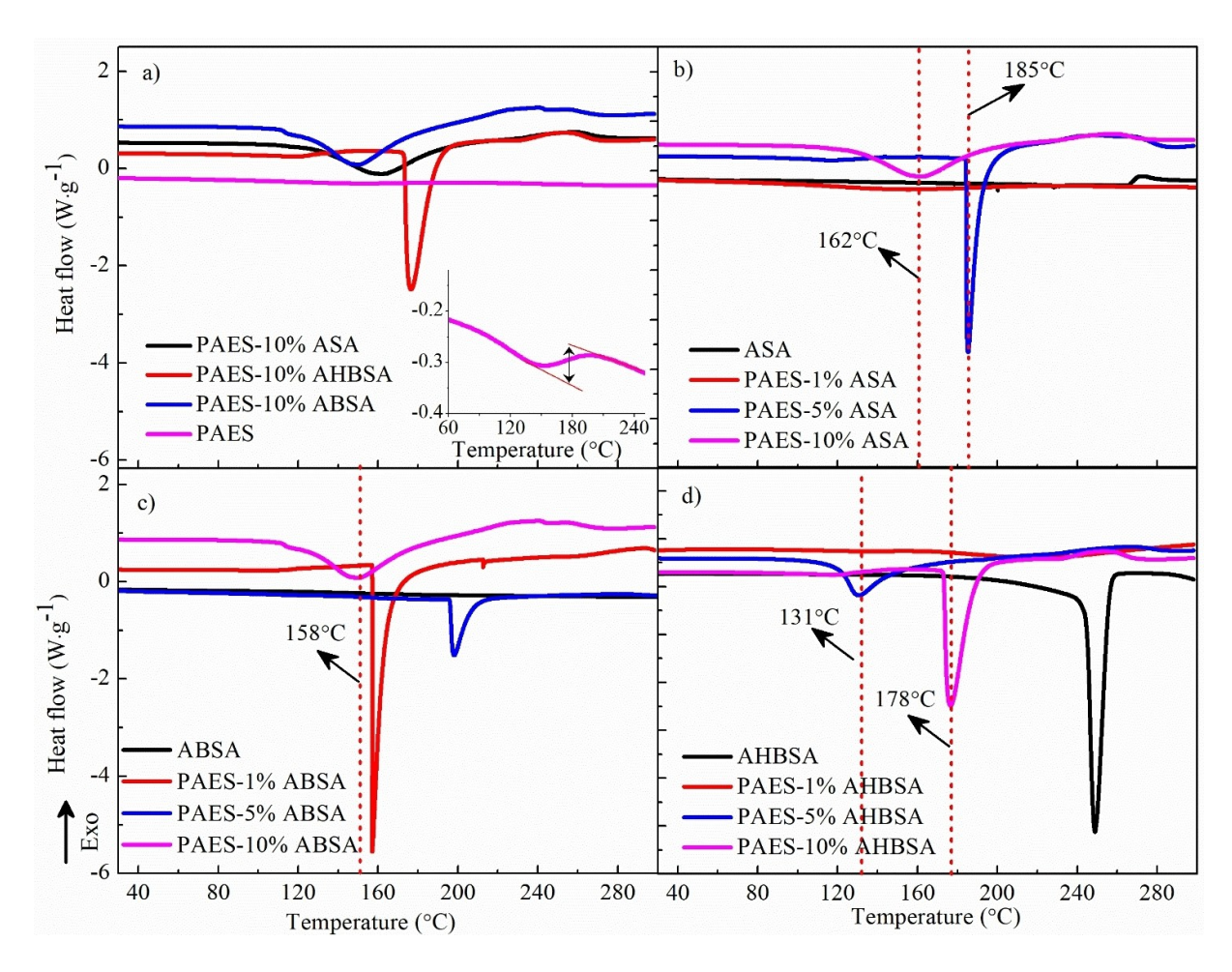


Figure 5. DSC curve of (a) pristine PAES and PAES-additive membranes with 10 vol.% concentration (inset shows the expanded view of PAES membrane), (b) ASA additive and PAES-ASA membranes, (c) ABSA additive and PAES-ABSA membranes and (d) AHBSA additive and PAES-AHBSA membranes at different additive concentrations

To understand the thermal properties of PAES membranes with additive concentration, DSC analysis of the PAES with ASA, ABSA and AHBSA content was also carried out and the results were compared with that of pure additives as well (Figure 5bd). As expected, pure ASA did not show any melting or glass transition temperature. However, a minor exothermic peak was observed at 266 °C which could probably be due to thermal decomposition of ASA to CO2 and CO gases. On the other hand, addition of 1 vol.% ASA did not bring any measurable change in the thermal curve. However, addition of 5 vol.% additive led to a very sharp melting peak at 185°C while their corresponding T<sub>a</sub> was observed at 170 °C. Though SEM do not show any phase segregation, further addition of ASA to 10 vol.% has led to broad peak with peak temperature observed at 162 °C (melting point). From the above observation it could concluded that the 5 vol.% ASA in PAES is the optimum concentration at which the PAES-ASA membranes could exhibit enhanced thermal behavior.

Similar studies were carried out with ABSA additives. Pure ABSA did not show any susceptible changes while AHBSA did show a sharp melting peak at 249 °C. PAES-1 %ABSA, PAES-5 % ABSA and PAES-10 %ABSA membranes had exhibited the

melting temperatures at 158, 198 and 149 °C, respectively. The  $T_{\alpha}$  peaks for PAES-5 %ABSA membrane was observed at 113 °C. These temperatures confirms that the addition of 5% ABSA has led to enhanced thermal stability of PAES compared to that of 1 and 10 vol.% ABSA additives. Figure 5d shows the effect of additive content on the DSC analysis of PAES-AHBSA membranes. From the chemical structure of AHBSA, it is understandable that AHBSA could form extra hydrogen bonds due to the presence of -OH and -NH2 groups in addition to -SO3H. In other words, addition of AHBSA additives would result in stronger bonds with PAES films compared to that of ASA and ABSA as the former is more susceptible to both inter and intramolecular hydrogen bonds. DSC analysis confirms that addition of 1 vol.% AHBSA additives to PAES do not bring any marked changes in their thermal properties and the derived membranes were found to behave similar to that of PAES (Figure 5d). However, PAES-5 %AHBSA and PAES-10 %AHBSA did show a melting of polymer membranes at 131 and 178 °C respectively. These results reveal that PAES with 10% AHBSA additives are much stable compared to that of PAES-1 %AHBSA and PAES-5%AHBSA membranes. These observations are in contrast to PAES-5 %ASA and PAES-5 %ABSA membranes.



However, it should be noted that the corresponding microstructure has a miscibility limit and therefore, it results in phase segregation in PAES membrane as shown in Figure 3. Overall, it could be concluded that the sulfonated additives are homogeneously blended with the PAES polymer and hence it has resulted in uniform microstructure (Figure 3). However, high concentration of AHBSA (say 10 vol.%) could result in phase segregation of additives with their sizes ranging between 1–2 μm. Further, the 5 vol.% addition of ASA and ABSA additives to PAES has helped to improve its thermal behavior compared to that of other compositions. In this study, it could be concluded that among all membranes PAES-10 %AHBSA was found to be best suited for high temperature PEM applications.

## Water uptake, Ion exchange capacity (IEC) and Leaching performance

Absorbed water plays an important role in determining the mechanism of proton conductivity and mechanical properties of the membranes in the fuel cell applications. It is well known that excess absorbed water content results in mechanically weak membranes, however, increased water uptake improves the transport properties of the solvated species which in turn enhances the proton conductivity. [6,30] Further, low water content in the membranes results in low electro-osmotic drag during fuel cell operation which results in low permeabilities.[31] Water uptake of PAES-additive membranes are shown in Figure 6a and in Table 1. Water performance tests were carried out using water at 25 °C. Figure 6a reveals that the water uptake in PAES-ASA membranes decreases with 1 vol.% addition of ASA additive (4.3 wt.%), however, further increase in the concentration of ASA has resulted in improved water uptake. On the other hand, PAES-ABSA showed linear decrease in water content. PAES-AHBSA was found to exhibit the inverse correlation to that of PAES-ASA membranes. The presence of hydroxyl group coupled with hydrophilic domain structure would have improved the percolation threshold within the PAES-AHBSA membranes. However, excess concentration of AHBSA additive (5 vol.% and above) would have altered the copolymer microstructure resulting in lowering of the water uptake capacity. The maximum water uptake observed for PAES-10%ASA, PAES-1%ABSA and PAES-10%AHBSA membranes were 8.2, 7.0 and 9.1 wt.%, respectively.

The ion exchange capacity (IEC) plays an important role in the swelling, proton conductivity and water uptake in PEM membranes. [32] IEC represents the number of protons that are replaced during the operating condition of the PEM membranes. [32] In general, increase in IEC helps not only to improve the performance of the PEM but also greater swelling in water. [33] IEC of PAES membranes and PAES-additive membranes are shown in Table 1 and in Figure 6b. IEC was only conducted at 25 °C. The measured IEC values of PAES-ASA, PAES-ABSA and PAES-AHBSA were in the range 0.26–0.48, 0.26–0.48 and 0.16–1.08 meq·g<sup>-1</sup>, respectively. As expected, the IEC values were found to increase linearly with additive concentration. The observed IEC values of pristine PAES membranes were slightly higher compared to that of PAES

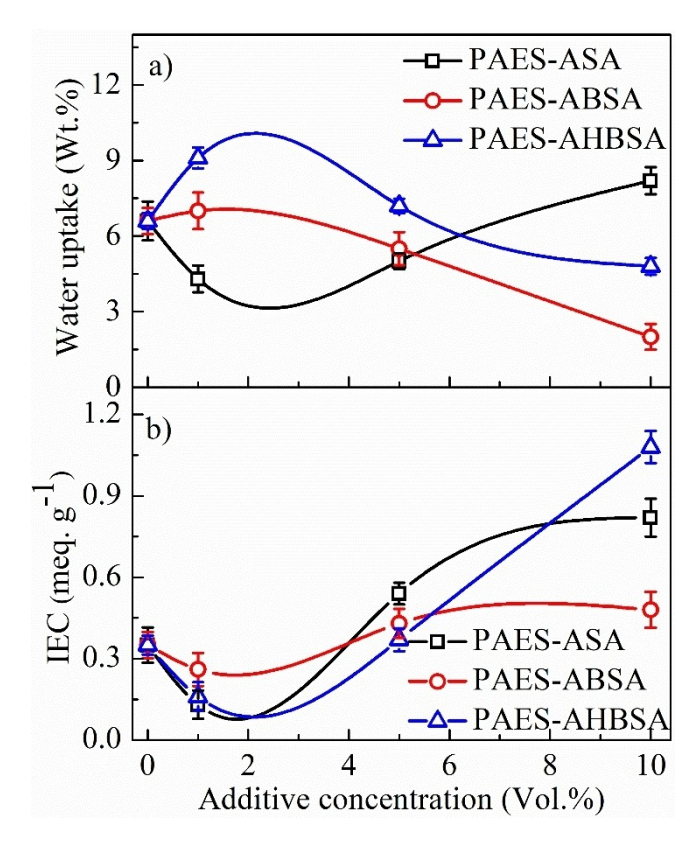


**Figure 6.** Variation of (a) water uptake (wt.%) and (b) IEC (meq·g<sup>-1</sup>) performance of PAES membranes at room temperature as a function of additive concentration

with 1 vol.% additives because of reduction in free volume in the polymer membranes during cross-linking. However, further increase in additive concentration resulted in overall increase in sulfonic acid group which in turn has improved their IEC. Among all membranes, PAES-10%AHBSA showed the highest IEC (1.08 meq. g $^{-1}$ ) followed by PAES-10%ASA membranes (0.82 meq. g $^{-1}$ ). Figure 6b shows that AHBSA had the most ion exchanges at the highest concentration and that its results were linear though the results increased greatly from 5 to 10 vol.% additives in PAES membrane.

Leaching occurred in all composite membranes as a result of the additives semi-soluble property in water (Figure 7b). ABSA membranes exhibited the lowest leaching performance at room temperature while the highest leaching percent was observed for the AHBSA films at high concentrations (10 vol.%). ASA films performed best in the water uptake tests as the percentages for all films remained low at all concentrations although its results were not linear. Table 2 shows the data cited in the literature on the PAES membrane derived from various methods. From the data it is eident that the water uptake and IEC in the range of 4–470 wt.% and 0.62–2.4 meq·g<sup>-1</sup>, respectively have been realized. From the data presented in Table 2 it is evident that water uptake and IEC varies and depends on the fabrication methodology. In the present study, it is amply demonstrated that the IEC of PAES-



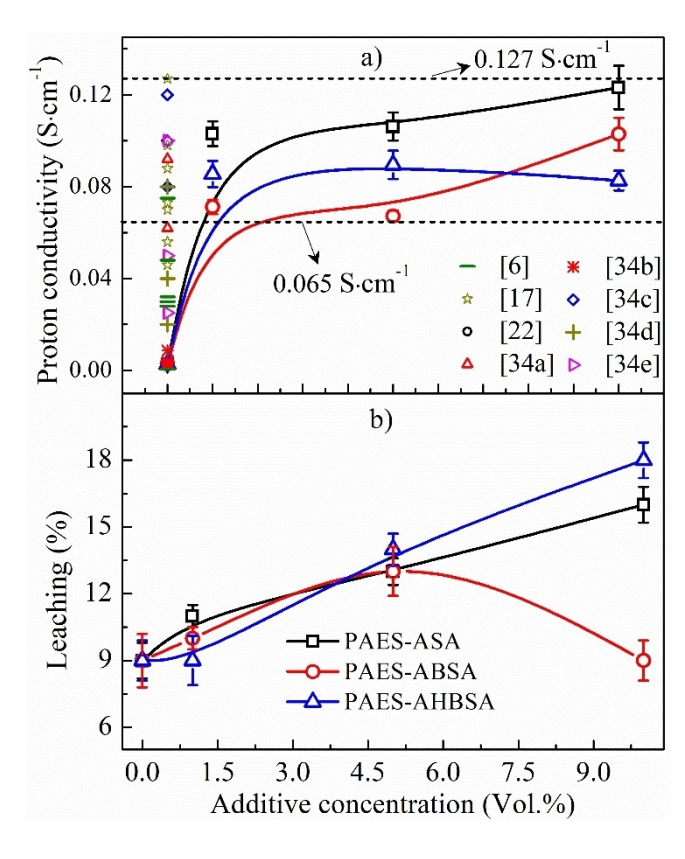


**Figure 7.** a) Comparison of proton conductivity values derived in this study (at 100% relative humidity at room temperature) with that of literature reported values<sup>[6,17, 22, 34]</sup> and b) Effect of additive concentration on the leaching effect in PAES and PAES-additive membranes

<b>Table 2.</b> Comparison of PAES membrane characteristics and proton conductivity reported in the literature									
S. No.	IEC (meq·g <sup>-1</sup> )	Water uptake (wt.%)	Conductivity (S·cm <sup>-1</sup> )	Reference					
1. 2. 3. 4. 5. 6. 7. 8. 9. 10. 11. 12 13. 14.	- 0.90-2.00 - 1.71-2.01 0.62-0.95 0.95-2.29 1.1-1.4 1.30-1.35 1.2 - 2.4 0.13-1.08 0.90 (Nafion® 212) (0.89) Nafion® 1135 (0.90)	4-240 18.3-327.4 20 51-76 10.9-14.1 40-470 25-66 - 16-19 - 25 2.0-9.1 24 38	0.66×10 <sup>-4</sup> -7.5×10 <sup>-2</sup> 0.056-0.127 2×10 <sup>-7</sup> -2×10 <sup>-3</sup> 0.062-0.092 2.5×10 <sup>-3</sup> -9.5×10 <sup>-3</sup> 0.08-0.32 0.02-0.08 0.025-0.10 0.004-0.083 0.07-0.09 0.0051 0.067-0.103 -	[6] [17] [22] [34a] [34b] [34c] [34d] [34e] [36] [23] [2] This study [34a] [34c] [34d]					
	Nafion® 112								

Where IEC- Ion exchange capacity. Proton conductivity values reported in Table 2 are from room temperature (RT) measurement. The suffixed numbers (say 212) of Nafion indicates the equivalent weight and thickness (inches) of extrusion-cast membrane.

additive membranes were overlapping with the literature reported values (Table 2).

#### **Proton conductivity**

Figure 7a shows the plot of proton conductivity of the membranes as a function of additive concentration measured at room temperature with 100% relative humidity. As expected, the lowest proton conductivity was observed in the unacidified PAES membranes due to the absence of the transport proton. In general, proton conductivity was found to increase gradually with the sulfonic acid additive concentration.[1b,2] It indicates that the hydrophilic domain clusters were increasing with sulfonation concentration, therefore, water entities were closer to each other resulting in improved conductivity.<sup>[2]</sup> It is well known that the proton conductivity of sulfonated membranes depends strongly on the type of charge carriers which in turn affects both water molecule presence and its clusters. [1a,b] Therefore, it is reasonable to suspect that increase in sulfonation group in PEM membranes would not improves the hydrophilic pathways but also broadens the contact point for the proton mobility.[1b,2] It is well documented that the proton conductivity in membranes follows two mechanisms viz., Grotthuss (hopping/jumping) and vehicle mechanism. [2] The former mechanism result in passing of protons along the chain of water molecules while in the latter mechanism, the proton combines with protonated vehicle (H<sub>3</sub>O<sup>-</sup> and CH<sub>3</sub>OH<sub>2</sub><sup>-</sup>) and an unprotonated H<sub>2</sub>O which in turn results in net transportation of the protons.<sup>[2]</sup> It was computed that the activation energy (E<sub>a</sub>) needed to undergo proton hopping mechanism ranges between 0.1 to 0.4 eV and that for vehicle mechanism requires greater than 0.5 eV.[2,35]

In this study, the proton conductivity of PAES composite membranes was shown to increase with all additive type and concentration evaluated. In PAES-ASA composites, the gradual increase in conductivity correlated with higher ASA additive concentration while higher concentration of ABSA and AHBSA membranes demonstrated no significant change above > 5 wt %. The overall, proton conductivity of PAES-ASA membranes were ranging between  $0.103 \pm 0.005$  to  $0.123 \pm 0.01 \text{ S} \cdot \text{cm}^{-1}$ . Among all membranes, PAES-10%ASA has exhibited the highest conductivity of  $0.123 \pm 0.01$  S·cm<sup>-1</sup> (Figure 7a). The increase in proton conductivity in PAES-ASA membrane could be due to enhanced degree of dissociation (acidity) caused by the presence of intramolecular hydrogen bonding between -SO<sub>3</sub>H and -NH<sub>2</sub>. Therefore, ASA addition helps to improve the degree of dissociation in PAES membrane which in turn enhances their proton conductivity.[36] On the other hand, PAES-5%ABSA exhibited the lowest conductivity value of  $0.067 \pm 0.002 \text{ S} \cdot \text{cm}^{-1}$ . This probably could be due to lower degree of dissociation as the interaction of ortho sulfonic acid (from ABSA) are reduced. However, as the concentration of ABSA reaches 10 vol.%, the proton conductivity was found to increase to  $0.103\pm$ 0.007 S·cm<sup>-1</sup> which could be due to the formation of ABSA clusters (phase segregation). Therefore, the interaction or degree of dissociation of -SO<sub>3</sub>H increases due to the formation of intermolecular H-bonding.[36] On the contrary, in PAES-



AHBSA membranes, AHBSA additives was found to have no impact/influence in the proton conductivity. It reveals that the presence of -OH group in AHBSA acts as a moderator and balances the extent of dissociation of sulfonic acid. Therefore, conductivity of PAES-AHBSA membranes remains unchanged even as the phase segregation of AHBSA takes place. The PAES-AHBSA membranes showed the proton conductivity values ranging between  $0.087\pm0.004$  to  $0.09\pm0.006~\text{S}\cdot\text{cm}^{-1}$ . The proton conductivity of pristine PAES membranes was found to  $\approx~2.74~\text{m}~\text{S}\cdot\text{cm}^{-1}$  which is lowest among all membranes prepared in this study.

From the above discussion, it is clear that the presence of sulfonated additives has a positive impact on the proton conductivity of the PAES membranes. ASA additives not only enhanced the proton conductivity of PAES membranes but it was found that the conductivity values increase with ASA concentration. Whereas increase in concentration of ABSA (1 and 5 vol.%) and AHBSA (1, 5 and 10 vol.%) additives in PAES membranes did not bring any substantial change in the proton conductivities. However, as the concentration of ABSA increased to 10 vol.% in PAES membranes, its proton conductivity was improved to  $0.103 \pm 0.007 \text{ S} \cdot \text{cm}^{-1}$ . Figure 7a and Table 2 shows the comparison of proton conductivity of PAES membranes derived in this study with that of literature reported values. In general, the proton conductivity values derived in this study are comparable to that of literature reported values (Table 2 and Figure 7a) and are in the range of 0.016 to 0.127 S·cm<sup>-1</sup>. These are indeed higher compared to some of the reported values (Table 2 and Figure 7a). Thus, it is amply demonstrated that the PAES-additive membranes derived in this study are thermally stable up to 400 °C and are highly proton conductivity.

#### Conclusion

Poly(arylene ether sulfone) (PAES) membranes with ASA, ABSA and AHBSA additives of concentration 1, 3 and 5 vol.% were successfully prepared using blending method. FTIR analysis confirmed the presence of sulfonic acid and ether linkage groups in the membranes. Thermogravimetric analysis (TGA) confirmed that the membranes undergo dehydration mass loss of around 1-2 wt.% due to the presence of extra bound water and intermolecular hydrogen bonding. Followed by two thermal events which were attributed to the sulfonic acid group mass loss (283 to 338°C) and rupturing of polymer backbone (beyond 340°C). Similarly, DSC analysis confirmed that the presence of additives in PAES delays the aromatic sulfonic acid degradation compared to that of pristine PAES membranes. Thermal analysis studies revealed that PAES-5% ASA, PAES-5%ABSA and PAES-10%AHBSA are best suited for the high temperature PEM applications compared to that of other additive concentrations. Microstructural analysis of PAESadditives confirmed that AHBSA with 10 vol.% additives result in phase segregation with their sizes ranging between 1–2  $\mu$ m. Proton conductivity study at 100% relative humidity revealed that PAES-ASA exhibited the highest conductivity of 0.123  $\pm$ 0.01 S·cm<sup>-1</sup>. Further, there was a gradual increase in conductivity with ASA concentration from  $0.103\pm0.005$  to  $0.123\pm$ 0.01 S·cm<sup>-1</sup>. This study further confirms that the degree of dissociation increases which is caused by intramolecular Hbonding. On the contrary, PAES-AHBSA membranes confirmed that the presence of -OH group in the additives acts as a moderator and helps to maintain the proton conductivity even at higher additive concentration (0.087  $\pm$  0.004 to 0.09  $\pm$ 0.006 S·cm<sup>-1</sup>). However, when leaching has to be considered PAES membranes with 1 vol.% ASA or PAES with 10 vol.% ABSA additives were found to be best suited. The best-balanced membrane was PAES-10%ABSA and PAES-1%ASA with high proton conductivity ( $\approx 0.103 \pm 0.07 \text{ S} \cdot \text{cm}^{-1}$  at 10 % RH, RT) and low leaching ability ( $\approx$ 10%). This study will serve as a guide for the fabrication of thermally stable and highly conductivity PAES membranes fuel cells with high sulfonated groups without sacrificing their mechanical properties.

#### **Supporting Information Summary**

Supporting information contains the thermogravimetry analysis of additives that are used in this study along with pristine PAES and PAES-additive membrane (Figure S1). Figure S1 shows that AHBSA exhibits two thermal events with first and second mass losses at around  $\approx 250\,^{\circ}\text{C}$  and  $300\,^{\circ}\text{C}$ , respectively. On the other hand, ASA and ABSA exhibits only single thermal event at around  $300\,^{\circ}\text{C}$ . These thermal analyses are overlapped with PAES-additives and pristine PAES membrane for comparative purpose (Figure S1b to Figure S1d). Similarly, a thermogravimetric comparison of pristine PAES with PAES-additive membranes with 10 vol.% additive concentration are shown in Figure S1a. Figure S2 shows the SEM images of PAES-additive membranes (PAES-ASA, PAES-ABSA and PAES-AHBSA) with 1 and 10 vol.% additives.

#### **Acknowledgements**

This project was supported by National Science Foundation Career Award (DMR-2006757); Florida Agricultural & Mechanical University, USA; Title III; Florida Agricultural & Mechanical University, USA. Proton conductivity experiments was supported by Virginia Polytechnic Institute and State University, USA. We thank the Department of Chemistry at Florida Agricultural & Mechanical University for FTIR characterization. Author would also like to thank Dr. Ramakrishnan and Dr. Sweat from FAMU-FSU College of Engineering and High Performance Materials Institute (HPMI) for the DSC and TGA facility. The authors also thank the members of the Arnett Polymer Research Group.

#### Conflict of Interest

The authors declare no conflict of interest.

#### **Data Availability Statement**

Research data are not shared.



**Keywords:** Fuel Cells · Poly(arylene ether sulfone) · Proton Conductivity · Proton Exchange Membranes · Sulfonated additives

- a) K.-D. Kreuer, S. J. Paddison, E. Spohr, M. Schuster, *Chem. Rev.* 2004, 104, 4637–4678; b) A. Kraytsberg, Y. Ein-Eli, *Energy Fuels* 2014, 28, 7303–7330; c) K. Kim, P. Heo, W. Hwang, J.-H. Baik, Y.-E. Sung, J.-C. Lee, *ACS Appl. Mater. Interfaces* 2018, 10, 21788–21793.
- [2] N. A. M. Harun, N. Shaari, N. F. H. Nik Zaiman, Int. J. Energy Res. 2021, 45, 19671–19708.
- [3] a) B. Bae, K. Miyatake, M. Watanabe, Macromolecules 2010, 43, 2684–2691; b) P. Khomein, W. Ketelaars, T. Lap, G. Liu, Renewable Sustainable Energy Rev. 2021, 137, 110471.
- [4] H. Tang, S. Peikang, S. P. Jiang, F. Wang, M. Pan, J. Power Sources 2007, 170, 85–92.
- [5] J. Zhang, Y. Tang, C. Song, J. Zhang, H. Wang, J. Power Sources 2006, 163, 532–537.
- [6] B. Liu, W. Hu, G. P. Robertson, M. D. Guiver, J. Mater. Chem. 2008, 18, 4675–4682.
- [7] M. C. Lopes de Oliveira, I. J. Sayeg, G. Ett, R. A. Antunes, Int. J. Hydrogen Energy 2014, 39, 16405–16418.
- [8] I. Petreanu, A. Marinoiu, C. Sisu, M. Varlam, R. Fierascu, P. Stanescu, M. Teodorescu, Mate. Res. Bull. 2017, 96, 136–142.
- [9] W. L. Harrison, M. A. Hickner, Y. S. Kim, J. E. McGrath, Fuel Cells 2005, 5, 201–212.
- [10] a) N. Y. Arnett, Virginia Polytechnic Institute and State University 2009;b) S. Fujiyama, J. Ishikawa, T. Omi, S. Tamai, *Polymer J.* 2008, 40, 17–24.
- [11] Y. S. Kim, M. A. Hickner, L. Dong, B. S. Pivovar, J. E. McGrath, J. Membr. Sci. 2004, 243, 317–326.
- [12] Y. S. Kim, L. Dong, M. A. Hickner, B. S. Pivovar, J. E. McGrath, *Polymer* 2003, 44, 5729–5736.
- [13] Y. S. Kim, F. Wang, M. Hickner, S. Mccartney, Y. T. Hong, W. Harrison, T. A. Zawodzinski, J. E. Mcgrath, J. Polym. Sci. Part B 2003, 41, 2816–2828.
- [14] P. Wang, X. Liu, D. Wang, M. Wang, D. Zhang, J. Chen, K. Li, Y. Li, K. Jia, Z. Wang, W. Feng, Q. Liu, J. Courtois, X. Yang, Mater. Res. Express 2021, 8, 122002
- [15] R. T. Tucker, C. C. Han, A. V. Dobrynin, R. A. Weiss, *Macromolecules* 2003, 36, 4404–4410.
- [16] H. Lee, J. Han, S. M. Ahn, H. Y. Jeong, J. Kim, H. Kim, T.-H. Kim, K. Kim, J.-C. Lee, ACS Appl. Energ. Mater. 2020, 3, 10495–10505.
- [17] Y. Zhang, Y. Wan, G. Zhang, K. Shao, C. Zhao, H. Li, H. Na, J. Membr. Sci. 2010, 348, 353–359.
- [18] M. Paul, H. B. Park, B. D. Freeman, A. Roy, J. E. McGrath, J. S. Riffle, Polymer 2008, 49, 2243–2252.
- [19] R. Jamal, F. Xu, W. Shao, T. Abdiryim, *Nanoscale Res. Lett.* **2013**, *8*, 117.
- [20] L.-M. Huang, T.-C. Wen, A. Gopalan, *Mater. Lett.* **2003**, *57*, 1765–1774.

- [21] G. Kalaiyarasan, A. V. Narendra Kumar, C. Sivakumar, J. Joseph, Sens. Actuators B 2015, 209, 883–888.
- [22] N. D. Sankir, R. O. Claus, J. B. Mecham, W. L. Harrison, Appl. Phys. Lett. 2005, 87, 241910.
- [23] H. Hou, F. Vacandio, M. L. D. Vona, P. Knauth, Electrochim. Acta 2012, 81, 58–63.
- [24] A. Ghosh, S. Banerjee, e-Polym. 2014, 14, 227–257.
- [25] D. S. Kim, K. H. Shin, H. B. Park, Y. S. Chung, S. Y. Nam, Y. M. Lee, J. Membr. Sci. 2006, 278, 428–436.
- [26] a) K. Oh, K. Ketpang, H. Kim, S. Shanmugam, J. Membr. Sci. 2016, 507, 135–142; b) L. Assumma, C. Iojoiu, G. Albayrak Ari, L. Cointeaux, J.-Y. Sanchez, Int. J. Hydrogen Energy 2014, 39, 2740–2750.
- [27] F. Wang, M. Hickner, Y. S. Kim, T. A. Zawodzinski, J. E. McGrath, J. Membr. Sci. 2002, 197, 231–242.
- [28] a) A. Mohamed, V. L. Finkenstadt, S. H. Gordon, G. Biresaw, D. E. Palmquist, P. Rayas-Duarte, J. Appl. Polym. Sci. 2008, 110, 3256–3266; b) G. D. Vilakati, E. M. V. Hoek, B. B. Mamba, Polym. Test. 2014, 34, 202–210.
- [29] a) M. J. Parker, in Comprehensive Composite Materials (Eds.: A. Kelly, C. Zweben), Pergamon, Oxford, 2000, pp. 183–226; b) N. Guigo, N. Sbirrazzuoli, in Handbook of Thermal Analysis and Calorimetry, vol. 6 (Eds.: S. Vyazovkin, N. Koga, C. Schick), Elsevier Science B. V., 2018, pp. 399–429.
- [30] P. Deivanayagam, A. Ramanujam Ramamoorthy, S. N. Jaisankar, *Polym. J.* 2013, 45, 166–172.
- [31] Q. Yan, H. Toghiani, J. Wu, J. Power Sources 2006, 158, 316-325.
- [32] P. Zheng, Q. Liu, Z. Li, D. Wang, X. Liu, Polymers (Basel). 2019, 11, 964.
- [33] S. M. MacKinnon, T. J. Fuller, F. D. Coms, M. R. Schoeneweiss, C. S. Gittleman, Y. H. Lai, R. Jiang, A. M. Brenner, in *Encyclopedia of Electro-chemical Power Sources* (Ed.: J. Garche), Elsevier, Amsterdam, 2009, pp. 741–754.
- [34] a) D. M. Yu, S. Yoon, T.-H. Kim, J. Y. Lee, J. Lee, Y. T. Hong, J. Membr. Sci. 2013, 446, 212–219; b) R. Guan, H. Dai, C. Li, J. Liu, J. Xu, J. Membr. Sci. 2006, 277, 148–156; c) H. Ghassemi, J. E. McGrath, T. A. Zawodzinski, Polymer 2006, 47, 4132–4139; d) Y. Li, A. Roy, A. S. Badami, M. Hill, J. Yang, S. Dunn, J. E. McGrath, J. Power Sources 2007, 172, 30–38; e) L. Assumma, H.-D. Nguyen, C. Iojoiu, S. Lyonnard, R. Mercier, E. Espuche, ACS Appl. Mater. Interfaces 2015, 7, 13808–13820.
- [35] Y. Ren, G. H. Chia, Z. Gao, Nano Today 2013, 8, 577–597.
- [36] Y. Kwon, S. Y. Lee, S. Hong, J. H. Jang, D. Henkensmeier, S. J. Yoo, H.-J. Kim, S.-H. Kim, *Polym. Chem.* 2015, 6, 233–239.

Submitted: September 12, 2022 Accepted: October 10, 2022